# Geology

## Early diagenesis of sulfur in a tropical upwelling system, Cabo Frio, southeastern Brazil

Rut Diaz, Manuel Moreira, Ursula Mendoza, Wilson Machado, Michael E. Böttcher, Helenice Santos, André Belém, Ramsés Capilla, Peter Escher and Ana L. Albuquerque

| | |
|---|---|
| **Email alerting services** | click www.gsapubs.org/cgi/alerts to receive free e-mail alerts when new articles cite this article |
| **Subscribe** | click www.gsapubs.org/subscriptions/ to subscribe to Geology |
| **Permission request** | click http://www.geosociety.org/pubs/copyrt.htm#gsa to contact GSA |

**Notes**

THE
GEOLOGICAL
SOCIETY
OF AMERICA

# Early diagenesis of sulfur in a tropical upwelling system, Cabo Frio, southeastern Brazil

Rut Diaz[1], Manuel Moreira[1], Ursula Mendoza[1], Wilson Machado[1], Michael E. Böttcher[2], Helenice Santos[1], André Belém[1], Ramsés Capilla[3], Peter Escher[2], and Ana L. Albuquerque[1]*

[1]Projeto Ressurgencia Team, Programa de Geoquímica Ambiental, Universidade Federal Fluminense, Outeiro São João Baptista s/n., Niterói RJ 24020-150, Brazil
[2]Geochemistry & Isotope Geochemistry Group, Marine Geology Section, Leibniz Institute for Baltic Sea Research Warnemünde, D-18119 Warnemünde, Germany
[3]Petrobras–Cenpes, Cidade Universitária, Ilha do Fundão, RJ 21941-915, Brazil

## ABSTRACT

The early diagenesis of sulfur was assessed in four short sediment cores on the continental shelf off southeastern Brazil that were deposited under the influence of an upwelling tropical system. This tropical upwelling area allows a direct focus on the coupled roles of hydrodynamic- and bioturbation-driven influences on sulfate reduction, sulfide re-oxidation and corresponding stable sulfur isotope signal formation. Under the depositional conditions of Cabo Frio, the degree of reactive iron pyritization was limited by both dissolved sulfide availability and pyrite oxidation events. Textural analyses of pyrite framboids provide evidence of re-oxidation processes, reflecting dynamic redox conditions in the sediments. The isotope composition of pore-water sulfate remained close to the modern seawater value, but very light stable sulfur isotope ratios ($^{34}S/^{32}S$) of chromium reducible sulfur (essentially pyrite) are found that reflect intense bioturbation-induced sulfur re-cycling. The sulfur isotope signatures developing in these tropical upwelling sites are similar to those of modern euxinic systems, although they are caused by a superimposition of sulfate reduction and an intense oxidative sulfur cycle.

## INTRODUCTION

The contents, speciation, and isotopic composition of sedimentary sulfur (S) species have been useful in evaluating early diagenetic processes in marine sediments, by revealing the coupling between the biogeochemistry of S with total organic carbon (TOC) and iron (Fe) cycling (e.g., Berner and Raiswell, 1983). In addition, the evaluation of stable isotope signatures of biogenic sulfides can help in elucidating the biogeochemical cycle of S, relating the sedimentary record of $\delta^{34}S$ to the composition of reduced S species (Wijsman et al., 2001; Hartmann and Nielsen, 2012). Therefore, many studies have evaluated S cycling in coastal areas owing to their high primary productivity and organic matter (OM) accumulation in sediments and in particular in sediments from upwelling areas, such as the Arabian Sea (Passier et al., 1997a), Namibia (Brüchert et al., 2003), Peru (Böning et al., 2004), and Chile (Böning et al., 2005; Zopfi et al., 2008). Moreover, textures and crystal sizes of pyrite ($FeS_2$) framboids may provide information about the dynamics of redox conditions in bottom waters and surface sediments (Wilkin et al., 1996). Less is known about the development of S isotope signals in tropical upwelling regions.

In southeastern Brazil, the continental shelf of Cabo Frio (Rio de Janeiro State) has received particular interest due to the occurrence of eddies and meanders of the Brazil Current, the influence of northeast winds, and the shelf physiographic features resulting in a complex hydrodynamic system (Calado et al., 2008). In order to provide a better understanding about the influences of oceanographic processes on the sedimentation conditions and corresponding cycling of S, carbon (C), and Fe, this study combines geochemical and stable isotope measurements with micro-textural analyses of pyrite. Our particular aim is to investigate the impact of intense re-oxidation of sulfide(s) on the development of sedimentary sulfur isotope signals.

## STUDY AREA AND METHODS

Four box-cores were collected across the shelf within a 680 km$^2$ mud bank (Fig. 1), formed by transgressive-regressive events during the Last Glacial Maximum, and favored by the position of the quasi-stationary Cabo Frio eddy. Sediment cores were sub-sampled by using PVC tubes (Ø = 10 cm, 40 cm length). The shelf-edge core BCCF10–01 (station 1) was collected at 142 m water depth and is mainly influenced by Brazil Current flow. Cores BCCF10–04 (station 4) and BCCF10–09 (station 9) were sampled at 120 m and 117 m water depths, respectively, within the middle-shelf area influenced by stationary and quasi-stationary cyclonic and anti-cyclonic eddy activity (Calado et al., 2008). The fourth core (BCCF10–15) was retrieved from the inner-shelf area (station 15) at 80 m water depth, influenced by wind-driven coastal upwelling. The oceanography of this region is dominated by the Brazil Current and the upwelling of South Atlantic Central Water (SACW), which increases local primary productivity and OM deposition, although water column oxic conditions are maintained (Pereira and Ebecken, 2009).

Pore-water was extracted by using the rhizon technique (Seeberg-Elverfeldt et al., 2005). Pore-water and sediment samples were processed within an $O_2$-free glove bag. Pore-water sub-samples were fixed with Zn-acetate for sulfide (Cline, 1969) and analyzed for sulfate content (Gieskes et al., 1991). The sediment cores were sliced in high resolution (1 cm) and fixed with Zn-acetate for acid volatile sulfides (AVS: FeS + $\Sigma H_2S$) and chromium reducible sulfur (CRS: $FeS_2 + S^0$) analyses. All samples were stored at 4 °C. TOC contents were analyzed on washed carbonate-free sediment and total sulfur (TS) was determined with a Eurovector elemental analyzer using Sn cups as sample containers and
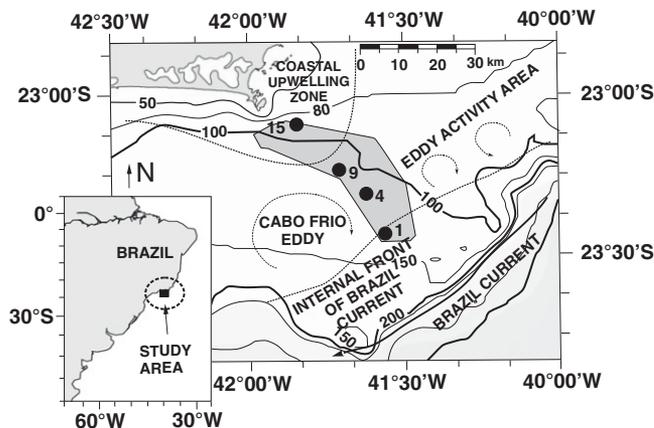


**Figure 1. Locations of study area and core sampling stations, showing their relative positions. Shaded area represents the mud bank.**

*E-mail: analuiza@geoq.uff.br.

$V_2O_5$ as a combustion catalyst. TOC contents were corrected for loss due to pre-measured dissolution of the carbonate fraction and subsequent salt washing off. AVS and CRS were determined in 1 g of sediment by a two-step distillation with cold 6 M HCl followed by boiling 2 M acidic $CrCl_2$ solution (Fossing and Jørgensen, 1989). The liberated $H_2S$ was collected in Zn-acetate (20%) traps, and its concentration was determined according to the method of Cline (1969). For stable S isotope analyses, the collected ZnS was converted to $Ag_2S$ with $AgNO_3$ solution, washed and dried. Pore-water sulfate for the isotope analysis was precipitated quantitatively as $BaSO_4$ by the addition of barium chloride, washed and dried. The isotope compositions of $Ag_2S$ and $BaSO_4$ samples were measured by means of combustion isotope-ratio-monitoring gas mass spectrometry (Thermo Finnigan™ MAT 253) coupled to a Thermo Flash elemental analyzer via a Conflo IV split interface. The isotope results are given in the usual $\delta^{34}S$ notation versus V-CDT (Vienna Canyon Diablo Troilite) (Mann et al., 2009). The degree of pyritization (DOP) was calculated from the reactive iron ($Fe_{react}$, 1 M HCl extractable) and pyritic iron ($Fe_{py}$, concentrated $HNO_3$ extractable) concentrations according to Huerta-Diaz and Morse (1990). Iron concentrations were analyzed by inductively coupled plasma–optical emission spectrometry (ICP-OES; HORIBA Jobin Yvon Ultima 2). A field emission scanning electron microscope (SEM-EDS; Philips XL 30) was used to examine the pyrite texture in freeze-dried samples and pyrite contents obtained by density separation (Wilkin et al., 1996). For further details, see the GSA Data Repository[1].

## RESULTS AND DISCUSSION

### Organic Carbon, Total and Inorganic Sulfur, and Iron Pyritization

The TOC contents (0.8% to 2.3%) are comparable to those from other upwelling areas (e.g., Passier et al., 1997a; Böning et al., 2005) and adjacent areas at the Cabo Frio coast (Burone et al., 2011). Below 8 cm depth, the cores from stations 4, 9, and 15 shows similar TOC contents (~2%), whereas the edge-shelf profile (station 1) has lower TOC (~1.4%) (Fig. 2A). Above 8 cm depth, the middle-shelf cores (stations 4 and 9) have the highest TOC contents, while shelf-edge and inner cores (stations 1 and 15) show a decreasing trend (Fig. 2A). A change in the Brazil Current transport strength and eddy formation over the shelf may explain the TOC sharp decrease in stations 1 and 15 corresponding to the upper 8 cm sediment layers. However, the higher values in stations 4 and 9 can be related to the constant action of the Cabo Frio stationary eddy favoring particulate matter settling.

The TS, CRS, and DOP values are relatively low, and showed an increase with depth at all stations (Figs. 2B, 2C, and 2G). This tendency of deeper pyrite accumulation is expected, since microbial OM decomposition via sulfate reduction leads to the production of $H_2S$ and subsequently iron sulfides (e.g., Berner and Raiswell, 1983; Passier et al., 1997a). The essentially constant pore-water sulfate concentrations at stations 1, 9, and 15 (25–28 mM; Fig. 2E) indicate low net sulfate reduction rates, as also supported by the non-detectable dissolved sulfide levels (<1 µM) found in all pore-water samples. The CRS concentrations vary from 0.05 to 0.3 wt%, while AVS was below the detection limit in most samples or detected at very low levels (≤0.01 wt%), which indicates that AVS has been re-oxidized and/or transformed into pyrite. Much lower CRS values in relation to TS suggest that some S entered into the organic matrix (Figs. 2B and 2C).

The DOP values provide a proxy of estimating the degree of bottom-water oxygenation (Raiswell et al., 1988), and they are also useful to identify the factors influencing pyrite formation in sediments (Berner and Raiswell, 1983). The DOP values of all cores are below 45% (Fig. 2G), which indicates that sediments were deposited under oxic water columns (Raiswell et al., 1988). The presence of SACW waters over the shelf is related to internal tide processes having a short residence time, thus explaining the oxic conditions of the bottom layers (Pereira and Ebecken, 2009). As deduced from the covariations with TS, the low DOP values suggest that pyrite formation was limited by the availability of sulfide (Fig. 3A).

The $Fe_{react}$ contents (35–140 µmol/g) correspond to the labile fraction of sedimentary iron that is available for pyrite formation (Suits and Wilkin, 1998) (Fig. 2H). These $Fe_{react}$ contents are fivefold higher than the $Fe_{py}$ contents (Fig. 2I), indicating that reactive Fe is not limiting the pyrite formation. No correlation between DOP and TOC was found in any of the cores, suggesting that DOP was not controlled by the OM contents. The TOC/CRS values are above the empirical TOC/CRS ratio for "normal" marine sediments (~2.8; Berner and Raiswell, 1983) (Fig. 3B). These high values support the assumption that TOC is not limiting pyrite accumulation, although they can be also explained by sulfide re-oxidation, caused by bioturbation, which was evident in the all box-cores, and possible contributions from sulfide-oxidizing bacteria (Böning et al., 2004). In addition, a low metabolizable OM fraction has been related to sulfide limitation, which can inhibit sulfate reduction and iron sulfide production (e.g., Berner and Raiswell, 1983), resulting in low pyritization.

### Pyrite Textures and Framboid Size Distribution

In the Cabo Frio shelf sediments, pyrite is predominantly found in the form of framboids, mainly associated with a clay mineral matrix. Framboidal pyrites showed crystalline appearances, infillings and secondary overgrowths, with cubo-octahedrons, octahedrons, and spheroidal morphologies of microcrystals (Fig. 4). Although framboids with diameters above 50 µm are rarely found (Wilkin et al., 1996), the framboid size from Cabo Frio sediments varied widely between 5 and 144 µm. Higher diameters
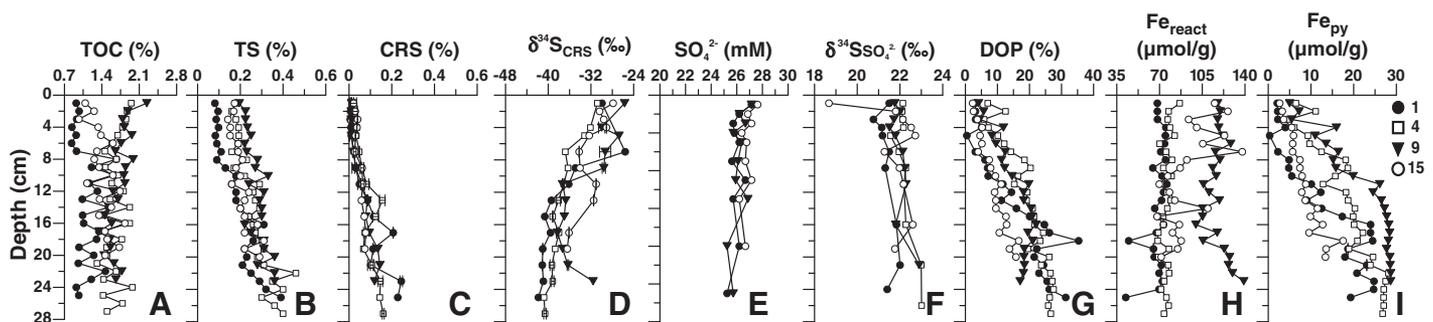


Figure 2. Downcore profiles. A: Total organic carbon (TOC). B: Total sulfur (TS). C: Chromium reducible sulfide (CRS). D: CRS stable isotopes ratio ($\delta^{34}S_{CRS}$). E: Sulfate concentration ($SO_4^{2-}$). F: Sulfate stable isotopes ratio ($\delta^{34}S_{SO_4^{2-}}$). G: Degree of pyritization (DOP). H: Reactive iron ($Fe_{react}$). I: Pyrite iron ($Fe_{py}$). Pore-water sulfide was not found analytically.

[1]GSA Data Repository item 2012250, methods, is available online at www.geosociety.org/pubs/ft2012.htm, or on request from editing@geosociety.org or Documents Secretary, GSA, P.O. Box 9140, Boulder, CO 80301, USA.
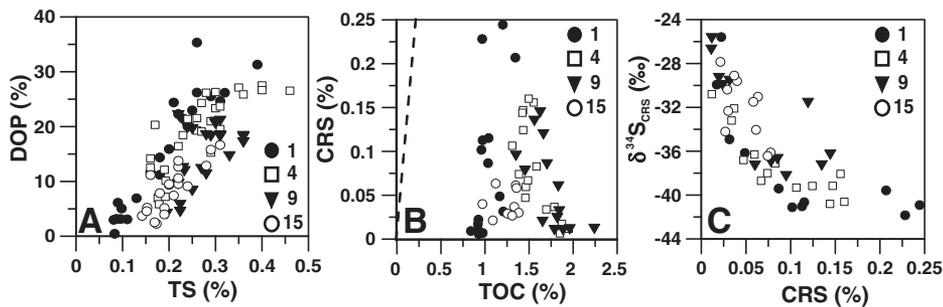
Figure 3. A: Relations of degree of pyritization (DOP) versus total sulfur (TS). B: Chromium reducible sulfide (CRS) versus total organic carbon (TOC) [dashed line represents average total organic carbon/chromium reducible sulfide (TOC/CRS) value for normal marine sediments; Berner and Raiswell, 1983]. C: CRS stable isotopes ratio ($\delta^{34}S_{CRS}$) versus CRS.
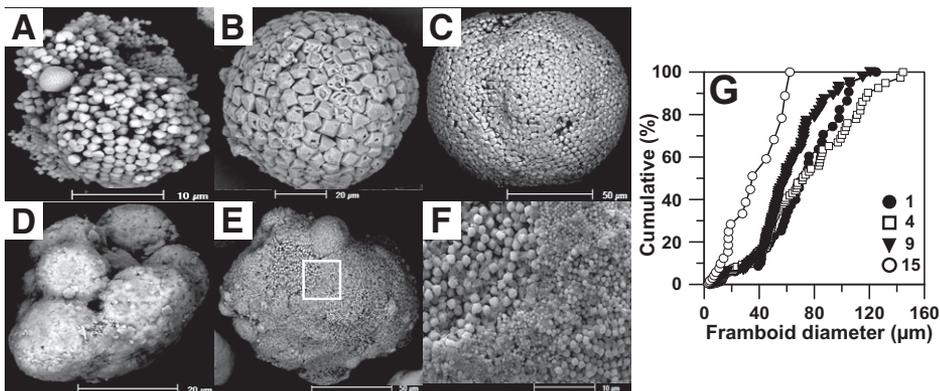


Figure 4. Backscattered scanning electron microscopy images. A: Pyrite framboid with secondary overgrowth. B: Pyrite framboid with cubo-octahedral crystals and evidence of oxidative dissolution pits on the surface. C: Large pyrite framboid with crystalline appearance. D: Polyframboid. E: Pyrite infillings and secondary crystal overgrowth on framboid aggregates. F: Detail of multistage crystal overgrowth shown in E. G: Cumulative size distributions.

has an S isotope composition of about +21‰ (Böttcher et al., 2007). The observed isotopic composition of pore-water sulfate is similar to seawater and does not vary much (Fig. 2F), indicating low levels of consumption versus rapid replenishment of sulfate via transport and/or sulfide re-oxidation in an essentially open system (Hartmann and Nielsen, 2012).

The pyrite formation in Cabo Frio sediments is associated with an isotope discrimination of 46‰ to 60‰ with respect to pore-water sulfate (Fig. 2D and F). High fractionations exceeding 47‰ have been explained by the multiple steps of S redox cycling. Following this approach, biogenic sulfide may be reoxidized to sulfur intermediates ($S^0$, $S_2O_3^{2-}$, $SO_3^{2-}$), followed by the bacterial disproportionation of intermediate S species (e.g., Jørgensen, 1990; Canfield and Thamdrup, 1994). This concept requires a continuous supply of oxidants and is ideally realized by the investigated sites at the Cabo Frio upwelling area. Therefore, the Cabo Frio setting provides a test case possibility for a previous model on the relation between intense S cycling and multi-step sulfur isotope fractionation (Canfield and Thamdrup, 1994). Field evidence of bioturbating *Aphrodita longicornis* polychaeta, the lack of sulfide and essentially constant sulfate concentrations in the pore-waters, as well as the texture of pyrite crystals gives evidence for re-oxidation in all sediment cores. These findings suggest an intense oxidative S cycling as an explanation for the observed fractionation. Aerobic and anaerobic degradation processes of pyrite (e.g., Schippers and Jørgensen, 2002) are possibly involved in such an oxidation step.

The CRS generally becomes more depleted in $^{34}S$ with increasing depth (Fig. 2D). The relation of $\delta^{34}S$ with CRS content for cores from stations 1 and 4 suggests that this depletion is greatest and becomes less variable for CRS contents exceeding ~0.1 wt%, with $\delta^{34}S$ values averaging −40‰ ± 1‰ (Fig. 3C). This apparent threshold for continuing partitioning change with increasing CRS concentration is probably associated with a higher stability of CRS in the deeper layers of the core from station 1, although this pattern was not observed for the core from station 4. Therefore, it is postulated that the possible re-oxidation effect was offset by comparatively higher CRS levels, which was not necessarily dependent on the depth (Fig. 2C). This trend was not found for less negative $\delta^{34}S$ data from cores at stations 9 and 15.

Besides the coupling between the reductive and oxidative parts in the sulfur cycle, sulfur isotope discrimination is also influenced by several other contributing factors, including the type of substrate fueling sulfate reduction (Kaplan and Rittenberg, 1964; Sim et al., 2011) and the structure of the active microbial sulfate-reducing community involved (Detmers et al., 2001; Sim et al., 2011). Kaplan and Rittenberg (1964) also

were found in cores from stations 1, 4, and 9 than in the core from station 15 (Fig. 4G). Individual microcrystal sizes ranged from 0.1 to 8 µm.

The low pyrite contents in the upper sediment layers of all cores are probably due to limitation of pyrite reactants for nucleation and growth (Wilkin and Arthur, 2001). This low content is supported by low CRS and DOP values (Figs. 2C and 2G). However, in the 2 cm and 6 cm depth of the station 15, pyrite was found as irregular masses (~130 µm) composed of framboid aggregates associated with euhedral crystals. These aggregates presented at least four different generations, each one with relatively uniform sizes (Figs. 4E and 4F). Wilkin et al. (1996) showed that different crystal sizes on a framboidal structure are typical of secondary growth over an earlier framboid.

Figure 4D shows an example of a polyframboid formed by processes of aggregation and fusion or welding of minor framboids (Sawlowicz, 1993). These processes, the successive crystal overgrowths (Fig. 4F) and the surface oxidation of pyrite grains (Fig. 4B) observed in Cabo Frio can be related to biological and/or physical sediment reworking. The bioturbation and physical sediment re-suspension can expose

the deeper sediment layers to more oxidizing condition before new burial. Infaunal activity, in addition, will create an array of dynamic redox gradients. During eddy incursions over the shelf, high productivity peaks promote fast particulate matter deposition, altering the bottom water $O_2$ content. However, it is expected that the constant intrusion of SACW with high $O_2$ concentration would maintain oxidizing conditions in the bottom layer of water column (Pereira and Ebecken, 2009).

The large sizes of framboid and their poly-generated growth indicate that pyrite formation occurred under a highly dynamic redox regime under strong biological and physical conditions, with abundant oxidants. Framboids formed under oxic or dysoxic conditions are larger and more variable in size than those formed under euxinic water conditions (Wilkin et al., 1996).

**Sulfur Isotopic Composition of Sedimentary Pyrite and Pore-Water Sulfate**

The isotopic composition of pyrite is dominantly controlled by the isotope discrimination that takes place during dissimilatory sulfate reduction (Chambers and Trudinger, 1979). Dissolved sulfate in the modern Atlantic Ocean

demonstrated that isotope fractionation may be related to the sulfate reduction rate, which may depend on electron donor type. We speculate that a combination of these factors may influence both the sulfate reduction rate and the observed vertical sulfur stable isotope patterns.

The S cycling under conditions of intense bioturbation and aerobic mineralization in the tropical upwelling Cabo Frio area leads to isotope signatures similar to those found in bacterial mat–controlled upwelling systems off the coast of Chile (Zopfi et al., 2008) or developed in euxinic sediments below water column redoxclines (Passier et al., 1997b; Wijsman et al., 2001).

## CONCLUSIONS AND IMPLICATION

The results of the sediment elemental, isotopic and textural analyses fully support that Cabo Frio shelf sediments were deposited under highly dynamic redox conditions in the surface layers beneath oxic bottom waters. Sulfur cycling appears to be a net effect of regional hydrodynamics and bioturbation that intensify its redox cycling, which together contribute to determine the extent of pyrite production and re-oxidation processes. Oxidation processes kept concentrations of pore-water sulfide, sedimentary CRS and DOP low. The low net sulfate reduction is suggested to result from sulfide-reoxidation and sulfate replenishing rates approximating the maximum gross sulfate reduction rate. High isotopic fractionation and pyrite textural characteristics, overgrowth and degradation signs were attributed to oscillations between more dominating reduction and re-oxidation processes. The results allow a more comprehensive evaluation of complex interactions of the hydrodynamics and bioturbation processes involved in the sulfur cycling near the sediment-water interface across this shelf and those expected to occur in other sedimentary environments under oxic conditions.

## REFERENCES CITED

Berner, R., and Raiswell, R., 1983, Burial of organic carbon and pyrite sulfur in sediments over Phanerozoic time: A new theory: Geochimica et Cosmochimica Acta, v. 47, p. 855–862, doi:10.1016/0016-7037(83)90151-5.

Böning, P., Brumsack, H., Böttcher, M.E., Schnetger, B., Kriete, C., Kallmeyer, J., and Borchers, S., 2004, Geochemistry of Peruvian near-surface sediments: Geochimica et Cosmochimica Acta, v. 68, p. 4429–4451, doi:10.1016/j.gca.2004.04.027.

Böning, P., Cuypers, S., Grunwald, M., Schnetger, B., and Brumsack, H., 2005, Geochemical characteristics of Chilean upwelling sediments at ~36° S: Marine Geology, v. 220, p. 1–21, doi:10.1016/j.margeo.2005.07.005.

Böttcher, M.E., Brumsack, H., and Dürselen, C.D., 2007, The isotopic composition of modern seawater sulfate: I. Coastal waters with special regard to the North Sea: Journal of Marine Systems, v. 67, p. 73–82, doi:10.1016/j.jmarsys.2006.09.006.

Burone, L., Sousa, S.H., Mahiques, M.M., Valente, P., Ciotti, A., and Yamashita, C., 2011, Benthic foraminiferal distribution on the southeastern Brazilian shelf and upper slope: Marine Biology, v. 158, p. 159–179, doi:10.1007/s00227-010-1549-7.

Brüchert, V., Jørgensen, B.B., Neumann, K., Riechmann, D., Schlösser, M., and Schulz, H., 2003, Regulation of bacterial sulfate reduction and hydrogen sulfide fluxes in the central Namibian coastal upwelling zone: Geochimica et Cosmochimica Acta, v. 67, p. 4505–4518, doi:10.1016/S0016-7037(03)00275-8.

Calado, L., Gangopadhyay, A., and Da Silveira, I.C.A., 2008, Feature-oriented regional modeling and simulations (FORMS) for the western South Atlantic: Southeastern Brazil region: Ocean Modelling, v. 25, p. 48–64, doi:10.1016/j.ocemod.2008.06.007.

Canfield, D.E., and Thamdrup, B., 1994, The production of $^{34}$S-depleted sulfide during bacterial disproportionation of elemental sulfur: Science, v. 266, p. 1973–1975, doi:10.1126/science.11540246.

Chambers, L.A., and Trudinger, P.A., 1979, Microbiological fractionation of stable sulfur isotopes: a review and critique: Geomicrobiology Journal, v. 1, p. 249–293, doi:10.1080/01490457909377735.

Cline, J.D., 1969, Spectrometry determination of hydrogen sulfide in natural waters: Limnology and Oceanography, v. 14, p. 454–458, doi:10.4319/lo.1969.14.3.0454.

Detmers, J., Brüchert, V., Habicht, K.S., and Kuever, J., 2001, Diversity of Sulfur Isotope Fractionations by Sulfate-Reducing Prokaryotes: Applied and Environmental Microbiology, v. 67, p. 888–894, doi:10.1128/AEM.67.2.888-894.2001.

Fossing, H., and Jørgensen, B.B., 1989, Measurement of bacterial sulfate reduction in sediments: Evaluation of a single-step chromium reduction method: Biochemistry, v. 8, p. 205–222.

Gieskes, J.M., Gamo, T., and Brumsack, H.J., 1991, Chemical methods for interstitial water analysis aboard JOIDES Resolution: ODP, Texas A&M University: Technical Note, v. 15, 60 p.

Hartmann, M., and Nielsen, H., 2012, δ$^{34}$S values in recent sea sediments and their significance using several sediment profiles from the western Baltic Sea, in Böttcher, M.E. and Hoefs, J., eds., Sulphur tales: A tribute on the occasion of the 90th birthday of Heimo Nielsen: Isotopes in Environmental and Health Studies, v. 48, p. 7–32.

Huerta-Diaz, M.A., and Morse, J.W., 1990, A quantitative method for determination of trace metal concentrations in sedimentary pyrite: Marine Chemistry, v. 29, p. 119–144, doi:10.1016/0304-4203(90)90009-2.

Jørgensen, B.B., 1990, A Thiosulfate Shunt in the Sulfur Cycle of Marine Sediments: Science, v. 249, p. 152–154, doi:10.1126/science.249.4965.152.

Kaplan, I.E., and Rittenberg, S.C., 1964, Microbiological fractionation of sulfur isotopes: Journal of General Microbiology, v. 34, p. 195–212.

Mann, J.L., Vocke, R.D., and Kelly, W.R., 2009, Revised δ$^{34}$S reference values for IAEA sulfur isotope reference materials S-2 and S-3: Rapid Communications in Mass Spectrometry, v. 23, p. 1116–1124, doi:10.1002/rcm.3977.

Passier, H.F., Luther, G.W., and de Lange, G., 1997a, Early diagenesis and sulphur speciation in sediments of the Oman Margin, northwestern Arabian Sea: Deep-Sea Research, v. 44, p. 1361–1380, doi:10.1016/S0967-0645(97)00014-3.

Passier, H.F., Middelburg, J.J., de Lange, G., and Böttcher, M.E., 1997b, Pyrite contents, microtexture, and sulfur isotopes in relation to the formation of the youngest eastern Mediterranean sapropel: Geology, v. 25, p. 519–522, doi:10.1130/0091-7613(1997)025<0519:PCMASI>2.3.CO;2.

Pereira, G.C., and Ebecken, N.F.F., 2009, Knowledge discovering for coastal waters classification: Expert Systems with Applications, v. 36, p. 8604–8609, doi:10.1016/j.eswa.2008.10.009.

Raiswell, R., Buckley, F., Berner, R.A., and Anderson, T.F., 1988, Degree of pyritization of iron as paleoenvironmental indicator of bottom-water oxygenation: Journal of Sedimentary Petrology, v. 58, p. 812–819.

Sawlowicz, S., 1993, Pyrite framboids and their development: a new conceptual mechanism: Geologische Rundschau, v. 82, p. 148–156, doi:10.1007/BF00563277.

Schippers, A., and Jørgensen, B.B., 2002, Biogeochemistry of pyrite and iron sulfide oxidation in marine sediments: Geochimica et Cosmochimica Acta, v. 66, p. 85–92, doi:10.1016/S0016-7037(01)00745-1.

Seeberg-Elverfeldt, J., Schlueter, M., Feseker, T., and Koelling, M., 2005, Rhizon sampling of pore waters near the sediment-water interface of aquatic systems: Limnology and Oceanography, Methods, v. 3, p. 361–371, doi:10.4319/lom.2005.3.361.

Sim, M.S., Bosak, T., and Ono, S., 2011, Large sulfur isotope fractionation does not require disproportionation: Science, v. 333, p. 74–77, doi:10.1126/science.1205103.

Suits, N.S., and Wilkin, R.T., 1998, Pyrite formation in the water column and sediments of a meromictic lake: Geology, v. 26, p. 1099–1102, doi:10.1130/0091-7613(1998)026<1099:PFITWC>2.3.CO;2.

Wijsman, J.W.M., Middelburg, J.J., Herman, P.M.J., Böttcher, M.E., and Heip, C.H.R., 2001, Sulfur and iron speciation in surface sediments along the northwestern margin of the Black Sea: Marine Chemistry, v. 74, p. 261–278, doi:10.1016/S0304-4203(01)00019-6.

Wilkin, R.T., Barnes, H.L., and Brantley, S.L., 1996, The size distribution of framboidal pyrite in modern sediments: An indicator of redox conditions: Geochimica et Cosmochimica Acta, v. 60, p. 3897–3912, doi:10.1016/0016-7037(96)00209-8.

Wilkin, R.T., and Arthur, M.A., 2001, Variations in pyrite texture, sulfur isotope composition, and iron systematics in the Black Sea: Evidence for Late Pleistocene to Holocene excursions of the $O_2$-$H_2S$ redox transition: Geochimica et Cosmochimica Acta, v. 65, p. 1399–1416, doi:10.1016/S0016-7037(01)00552-X.

Zopfi, J., Böttcher, M.E., and Jørgensen, B.B., 2008, Biogeochemistry of sulfur and iron in *Thioploca*-colonized surface sediments in the upwelling area off central Chile: Geochimica et Cosmochimica Acta, v. 72, p. 827–843, doi:10.1016/j.gca.2007.11.031.